Engineering Notes

ENGINEERING NOTES are short manuscripts describing new developments or important results of a preliminary nature. These Notes cannot exceed 6 manuscript pages and 3 figures; a page of text may be substituted for a figure and vice versa. After informal review by the editors, they may be published within a few months of the date of receipt. Style requirements are the same as for regular contributions (see inside back cover).

Mariner 10 Star Photography

T. E. Thorpe*
Jet Propulsion Laboratory, Pasadena, Calif.

SHORTLY after launch of the Mariner 10 spacecraft (November 5, 1973), a serious malfunction of both telescope heaters raised concern about the possibility of abnormal optical performance. The tiny instrument transducers indicated that temperatures on the telescope front optics had dropped below preflight test calibration (-17°C) and that the camera head was at least -5°C. Both the temperature and temperature differential (front to back of telescope) could have affected telescope focus and camera sensitivity. Two series of star photographs were immediately scheduled to precede the later scan platform pointing calibrations. On November 6 and 8, over 100 frames of the Pleiades star field were recorded to determine the adequacy of instrument performance towards fulfilling planned mission objectives. These data, in addition to complementing subjective and edge-trace analysis of Earth and the Moon images, provided information relative to camera focus, light transfer, detection thresholds, geometric distortion, noise, and limit cycle motion.

Among the scientific instruments carried aboard the spacecraft for the reconnaissance of Venus and Mercury were two identical television cameras, each having a long (1500 mm) and short (62 mm) focal-length capability. These telescopes were used in conjunction with a filter-wheel assembly which could be commanded to one of eight positions and a focal-plane shutter to provide an image on a slow-scan vidicon tube. Each TV frame consisted of 700 scan lines with each scan line from the vidicon sampled 832 times (called picture elements or pixels). These samples were encoded to 256 discrete levels (8 bits) and routed to the spacecraft data system for either storage and/or direct transmission to Earth. One television frame was read out every 42 sec. For purposes of redundancy and because a significant amount of time (approximately 30 sec) was used to prepare the vidicon photosurface for its next picture, two cameras were employed with one camera reading out its image while the other was being prepared.

Table 1 lists some of the important parameters of the Mariner 10 television instrument. The long focal length camera is similar to one of two cameras planned for the Mariner Jupiter-Saturn (MJS) mission to be launched in 1977. Hence, the instrument performance was closely monitored.

The anticipated Mariner 10 image response to stars was thought to be as good as the Mariner 9 narrow-angle television instrument. This is because the smaller aperture of Mariner 10 was compensated by increased optics transmission and the potential use of a clear filter (filter factor = 1.08) instead of the previously used minus-blue B-camera filter (filter factor = 2.5). Similar optical point-spread functions were also achieved by virtue of the nearly diffraction-limited Mariner 10 telescope design (50% vs 62% image modulation at 33 lp/mm, Mariner 9 vs Mariner 10).

Table 1 Optical characteristics of the Mariner 10 cameras

Characteristic	Cameras A and B narrow angle	Cameras A and B wide angle
Focal length	150 cm	6.2 cm
Focal ratio	f/8.43	f/12
T-number	*T*/12	*T*/18
Angular field of view	0.48° × 0.37°	11° × 14°
Nominal shutter operation	3 ms TO 12 sec	3 ms TO 12 sec
Scan lines per frame	700	700
Picture elements per line	832	832
Bits per picture element	8	8
Angle subtended by TV line	9μ rad	230μrad
Frame time	42 sec	42 sec
Filters (effective active wavelength)	360,362,476,519 483, 554 nm	515nm

Reference 1 describes the behavior of the Mariner 9 B-camera response to point sources from pre-flight calibration through mission star photography from Mars orbit. However, the difference in focal lengths implied that the instrument was three times as sensitive to image motion (i.e., a stellar image remained on a picture element only one-third as long as the image on a Mariner 9 record).

Results

Profiles of star images in both television line and sample direction yielded point-spread functions which were sensitive to cameras focus. Unfortunately, direct interpretation was affected by scplatform motion (image smear). Figure 1 displays the appearance of both a pinhole and a +4th magnitude star photographed by the A and B cameras with 0.52 and 1.04 sec exposures and ×3 magnitude star recorded with an 11.7 sec shutter speed. The corresponding image motions during the star photography were 1.0, 1.9, and 17 picture elements (pixels); the result of a large spacecraft attitude drift rate. Figure 2 shows typical pitch, yaw, and roll motions for two data-taking periods. The corresponding rates (slopes) were then projected into the image format based on the camera-pointing direction (cone: 165°; clock: 266° [Canopus], 100° [Vega]). Typical rates varied from 10-25 μr/sec (1.1-2.8 pixels/sec).

Many examples of nonuniform attitude-drift motion were evident by the star trails contained in pictures exposed at 11.7 sec. The comparatively long focal-length telescopes could reveal motion changes of less than 1 μr/sec with amplitudes of $<10\mu$ across the vidicon faceplate. In a few cases, very regular differences of motion typical of a small sinusoidal vibration are apparent. Specifically, pictures taken immediately after reaching the Pleiades pointing direction on November 8 (FDS 10560-10570) showed a gradually decreasing regular motion variation (Fig. 3); i.e., as shown in Table 2.

A suggestion of an even lower frequency (0.3 cps) vibration was also indicated by a slightly brighter pulse every third maximum signal. Because the maxima appeared most distinct with vertical (line) trails, this motion variation was best modeled by vibration along the pixel direction (across trail length). Hence, vibration in the pitch or cross-yaw direction was indicated.

Received May 22, 1974; revision received January 17, 1975. This paper presents the results of one phase of research carried out at the Jet Propulsion Laboratory, California Institute of Technology, under NASA Contract NAS 7-100.

Index categories: Data Sensing and Presentation or Transmission Systems; Spacecraft Navigation, Guidance, and Flight-Path Control Systems.

*Photoscientist, Space Sciences Divison.

LS →

CAMERA A

FDS 10595 0.5 sec						FDS 6661 1.04 sec						10μ PINHOLE					
1	1	1	1	1	1	6	6	6	6	7	6	2	7	28	17	3	3
1	20	37	16	2	1	6	6	16	12	6	6	4	38	66	27	4	1
1	7	38	34	3	1	6	32	95	32	6	6	3	43	67	33	5	2
1	2	21	17	2	1	6	17	39	13	8	2	3	16	52	33	4	2
1	1	4	7	3	1	6	8	13	10	7	6	2	4	23	24	3	3
1	1	1	2	1	1	6	7	7	8	6	6	1	2	4	7	5	3

19 TAURI
+4.4

CAMERA B

FDS 10590 0.5 sec							FDS 6660 1.04 sec							10μ PINHOLE						
3	2	2	2	3	2	3	1	1	1	1	1	1	1	6	6	6	7	6	6	6
2	4	3	3	9	4	2	1	1	1	5	21	27	4	7	7	7	8	8	6	7
3	3	13	72	17	2	1	1	1	9	68	103	23	1	7	7	31	51	25	8	7
2	6	'61	48	8	4	2	1	4	65	109	59	13	3	6	8	43	80	31	8	7
2	19	61	18	10	4	3	1	23	84	70	20	6	3	7	8	34	42	13	9	6
2	8	18	13	6	3	2	1	5	28	24	11	4	2	7	7	12	14	11	7	7
3	3	7	6	4	3	2	1	1	5	9	6	2	1	6	6	8	8	8	6	6

19 TAURI
+4.4

CAMERA A

FDS 10641 11.7 sec

2	3	5	5	5	3	3	3	4	3	3	2	3							
3	6	14	16	14	11	8	5	4	4	3	3	2							
3	5	11	15	14	16	16	16	14	10	7	6	3	3	3	3	3	2	2	
3	5	7	11	13	14	15	16	16	16	17	16	13	10	7	5	4	3	3	3
2	2	4	5	6	8	9	13	13	15	15	16	16	17	16	15	11	6	3	2
3	2	3	3	4	4	4	5	7	9	11	13	15	15	15	16	14	8	3	3
2	2	3	3	2	3	3	3	3	4	5	5	7	9	11	13	15	10	5	3
										3	2	4	5	4	7	7	7	5	4
										3	3	3	3	3	4	4	4	2	2

+6.3

Fig. 1 Camera B Pleiades picture #10562 (11.7 sec). Contours: 10 DN, 50% DN Max, 100 DN.

Table 2 Vibration induced star trail maxima vs picture (FDS)#

FDS	#Maxima	Spacing	Frequency	Amplitude Vidicon
10563	9	10 pixels	0.77 cps	143μ
10566	9	4 pixels	0.77 cps	55μ
10567	9	2.5	0.77 cps	34μ
10569	?	≤1 pixel	?	<10μ

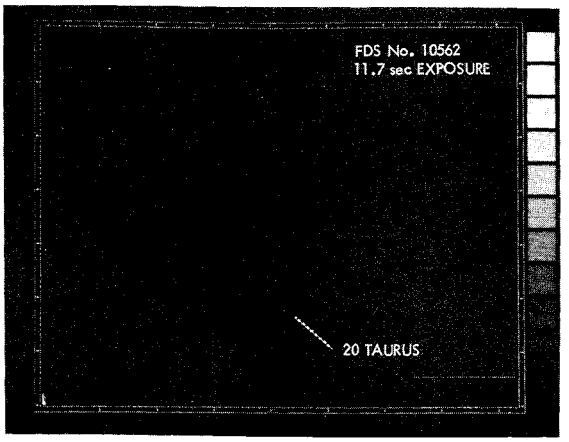

Fig. 3 Typical star images.

Despite this movement, comparison with preflight measurement suggested little, if any, change in optical image size had occurred. Close examination reveals a slightly narrower profile for Camera A in both horizontal and vertical directions. Fourier transforms of these curves corrected for image motion differences confirmed a higher Camera A MTF response at high spatial frequencies compared with Camera B. The approximate resolution difference (modulation) at 0.35 cycles/sample was 20%.

Limiting stellar magnitude and geometric angular measurement are also parameters basic to the prediction of navigation accuracies.

A. Sensitivity

The light transfer characteristics of the Mariner cameras as illustrated by the maximum data number (DN) per stellar magnitude again depended on image motion; i.e., the time an image remains on a given pixel. Also, the variance of star image data numbers was due to a combination of three primary effects: target exposure, image motion, and image size (point spread). Second-order effects, such as: random noise, camera shading, geometric distortion, smear azimuth with respect to frame axis, and bit error rates also influenced the relative signal. Table 3 indicates the relative magnitude of

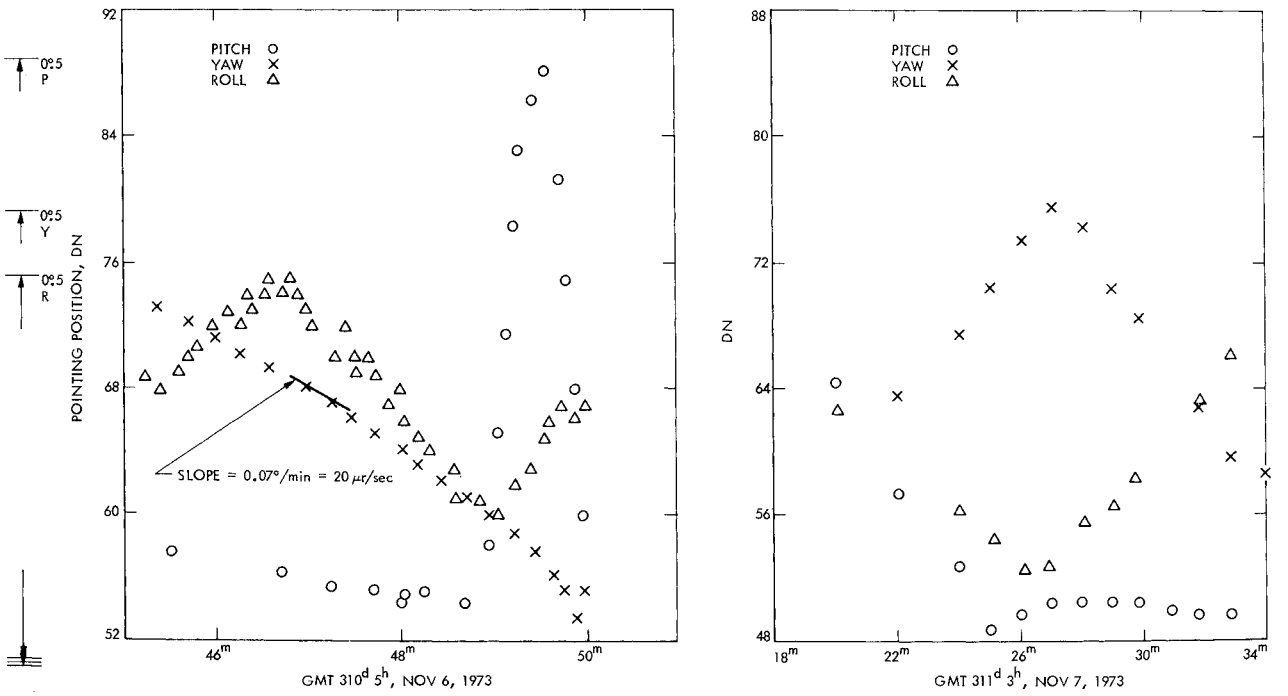

Fig. 2 Typical spacecraft attitude drift motion.

Table 3 Star image frame-to-frame consistency

Characteristic	Camera A	Camera B
Mean maxima (0.5 sec)	205 DN	186 DN
Mean ΣDN	985 DN	1142 DN
Random dispersion (sky)	0.6 DN	0.75 DN
Maxima dispersion (rms)	27 DN (13%)	10 DN (5.5%)
ΣDN dispersion (rms	34 DN (3.5%)	14 DN (1.2%)
Image motion variation (rms)	8.5%	27%
Image motion variation (pixels)	0.11	0.42
Sky dispersion for image locations (shading)	0.4 DN	0.2 DN
Integrated sky sample dispersion (rms)	7 DN	3 DN

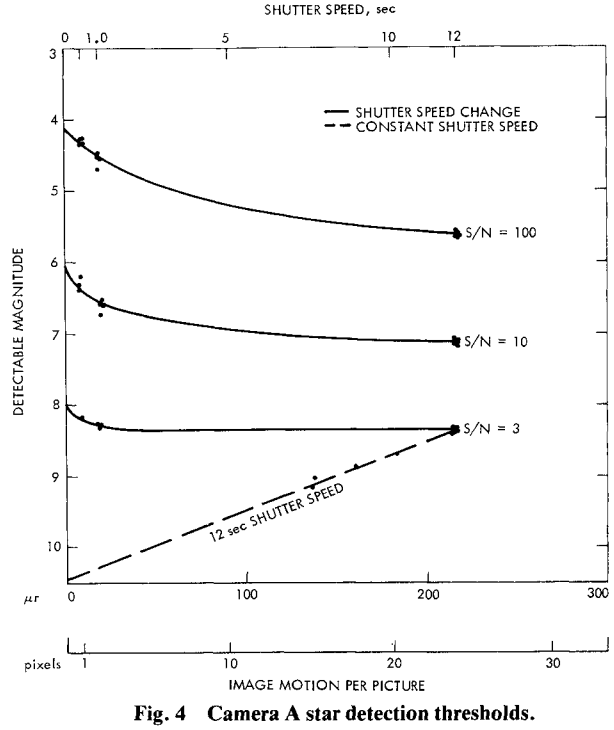

Fig. 4 Camera A star detection thresholds.

these dispersions: Star - 17 Tauris; magnitude - +3.8; number of frames - 10.

Although Camera B had larger random noise and slightly less high frequency response (smaller signal maxima), the signal-to-dispersion ratio was nevertheless higher than Camera A for midscale exposures ($S/D = 7.6$ A; 18.6B).

Because the Camera A telescope concentrated more photons into a smaller area, this instrument maintained the lowest detection threshold (by nearly a stellar magnitude) at short shutter speeds. However, when exposures were of several seconds duration, the larger diameter point-spread function (with smaller maxima) produced by Camera B resulted in easier image recognition. Figure 4 illustrates this relationship. The dashed line refers to signal level as a function of image motion for a 12-sec shutter speed; whereas, the solid lines reflect the combination of incident energy change and image displacement as a function of shutter speed at a constant drift rate of $20\mu r$/sec.

B. Focal Length and Geometric Distortion

The line and sample picture coordinates of stars of known angular separation provided scale factors and focal lengths for each camera. The calculated values reflect geometric distortion and image center finding errors. By converting line and sample coordinates to displacement on the vidicon faceplate in millimeters using preflight calibration relations,

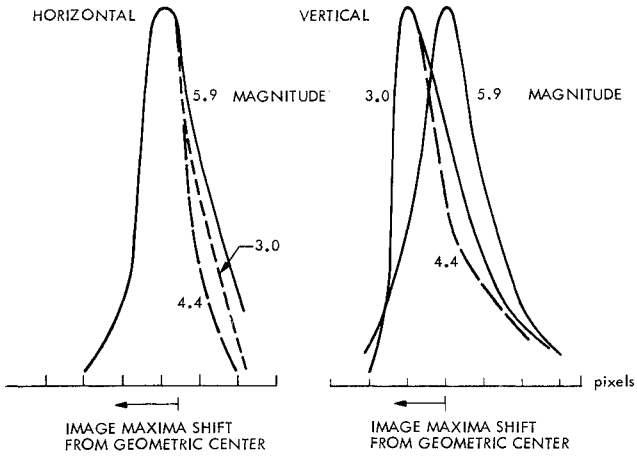

Fig. 5 Camer A normalized star image profiles.

the relative focal lengths were found to be: 1432 mm (Camera A) and 1442 mm (Camera B). These values differ from the preflight measurements of 1495.7 mm and 1503.7 mm, respectively, and indicated geometric distortion amounting to -4% over typically 320 pixel image separations.

Both partial image erasure and charge bias within the vidicon readout produced an asymmetrical profile of star images. Such displacement resulted in geometrical uncertainties of up to several TV lines for very bright stars. Figure 5 shows the effect for Mariner 10 Camera A star profiles normalized at the maximum DN.

Conclusions

The Mariner 10 TV Subsystem operation was consistent with preflight measurement to within observable accuracies. Geometric distortion and noise analysis suggest apparent thresholds which limited optical navigation accuracies.

Several differences between Cameras A and B have been described that affected encounter sequence strategy. Camera A obtained the highest spatial resolution, and planetary surface photography demanding highest response emphasized use of this camera. Conversely, Camera B yielded integrated brightness values; e.g., planet approach photometry, with less dispersion, and provided the most sensitivity for long exposures; e.g., beyond terminator atmospheric scattering.

Of major importance are the implications of this photography to future Mariner outer planet missions utilizing similar cameras. Spacecraft attitude control using cold gas jet stabilization may reduce navigation accuracies and the early detection distances of satellites if drift rates of $5\mu r$/sec or less cannot be achieved. Figure 4 showed a 3 magnitude sensitivity loss at $20\mu r$/sec or a minimum practical shutter speed of 1 sec for star photography. Perhaps special schemes such as driving the platform to the edge of its deadband while the spacecraft is gyro stabilized could justify the use of longer exposures.

Science use of this instrument to look for faint sources, e.g., small bodies, extended atmospheres, and particulate clouds, is difficult at 1.5 m focal lengths. Although it may be argued that the choice of this sensor and telescope focal length has resulted in an instrument lacking some sensitivity for outer planet missions, the addition of image motion to the inherent camera uncertainties further makes photometry of point sources impossible. This result could make it difficult for MJS to obtain in-flight verification of instrument performance and seriously affect optical navigation.

References

[1]Thorpe, T. E., "Mariner 9 Star Photography," *Applied Optics*, Vol. 12, Feb. 1973, pp. 359-363.

[2]Thorpe, T. E., "Verification of Performance of the Mariner 9 Television Cameras," *Applied Optics*, Vol. 12, Aug. 1973, p. 1775-1784.